

# Experimental study of the effect of strong shock heated test gases with cubic zirconia

V. Jayaram<sup>1\*</sup>, K. P. J. Reddy<sup>2</sup>

<sup>1</sup>*Shock Induced Materials Chemistry Lab, Solid State and Structural Chemistry Unit, Indian Institute of Science, Bangalore 560012, India*

<sup>2</sup>*Laboratory for Hypersonic and Shock Wave Research, Department of Aerospace Engineering, Indian Institute of Science, Bangalore 560012, India*

\*Corresponding author, Tel: (+91) 9845770188; E-mail: jayaram@sscu.iisc.ernet.in, drjayaramv@gmail.com

Received: 23 December 2015, Revised: 13 February 2016 and Accepted: 10 November 2016

DOI: 10.5185/amlett.2017.6379

www.vbripress.com/aml

## Abstract

This paper presents a novel method of interaction of zirconia with strong shock wave in presence of dissociated/non-dissociated gas species for short duration using shock tube. Cubic zirconia (c-ZrO<sub>2</sub>) was synthesized by solution combustion method and exposed to strong shock heated N<sub>2</sub> and O<sub>2</sub> test gases in a free piston driven shock tube (FPST). FPST is used to heat the test gases to very high temperature of about 7540-9530 K (estimated) and reflected shock pressure of about 65-70 bar for short duration (2-3 ms). X-ray diffraction (XRD) study shows the phase transformation of c-ZrO<sub>2</sub> to m-ZrO<sub>2</sub>. Scanning electron microscopy (SEM) images shows the formation of sharp nano/micro zirconia needles due to melting and nucleation during super heating and cooling at the rate of about 10<sup>6</sup> K/s. These types of sharp nano/micro needles are observed for the first time in this shock tube experiment. X-ray photoelectron spectroscopy (XPS) and Fourier transform infrared (FTIR) spectroscopy show no change in electronic structure and chemical composition of ZrO<sub>2</sub> which indicates that the reaction is fully catalytic. This unique experimental methodology can be used to study the chemistry of materials under extreme thermodynamic conditions which is of seminal importance in space, nuclear and other high temperature applications. Copyright © 2016 VBRI Press.

**Keywords:** Phase transformation, shock heated gas, gas-solid interaction, nano/micro zirconia needles, aerothermodynamic reactions.

## Introduction

Thermal barrier coating (TBC) materials are used in traditional and advanced applications due to their high melting point, good mechanical properties and chemical inertness. Atmosphere re-entry produces extremely high temperature shock waves, causing dissociation of air (O<sub>2</sub> and N<sub>2</sub>), taking them to a non-equilibrium state. When the gas flow is in non-equilibrium state dissociated gas recombines at the third body, which causes the increase in surface temperature of the materials. To prevent recombination of dissociated atoms, TBC materials with low catalytic properties are required. Study of both homogeneous and heterogeneous catalytic reactions is important to understand interaction of materials with high enthalpy gases. Properties of different TBC materials and mullite were reported in the literature [1, 2]. One such TBC material like zirconia (ZrO<sub>2</sub>) is extremely good for aerospace, nuclear and high temperature applications. It offers chemical and corrosion inertness to temperatures well above the melting point of alumina. At very high temperatures (>2650 K) zirconia has a cubic (c) structure and at intermediate temperatures (1450 to 2650 K) it has a tetragonal (t) structure [3, 4]. Monoclinic (m) structure is formed when the temperature is less than 1450 K [5, 6]. During the tetragonal to monoclinic transformation all

structural parameters show linear temperature dependence. Strong non-linearity was found in the transformation from m to t direction. This shows that the parameters of the tetragonal structure are not a unique function of temperature, but all parameters of the monoclinic phase have normal linear temperature dependence in its ranges of existence [7]. An analysis of temperature factors suggests dynamical disorder in the tetragonal phase and static disorder in the monoclinic phase. Cubic zirconia has a fluorite structure in which Zr<sup>4+</sup> ion is surrounded by eight O<sup>2-</sup> ions positioned at the vertices of a cube, whereas each anion is surrounded by four Zr<sup>4+</sup> ions positioned at the vertices of a tetrahedron [8]. Both the tetragonal (t-ZrO<sub>2</sub>) and monoclinic (m-ZrO<sub>2</sub>) structure can be considered as distortions of the cubic structure. A shift of the oxygen atoms along the crystallographic c-axis leads to the formation of the tetragonal structure with a consequent change in lattice parameters. In the monoclinic phase, the coordination number of Zr<sup>4+</sup> is 7 and O<sup>2-</sup> has the coordination numbers of 3 and 4. Formation of m-ZrO<sub>2</sub> phase occurs while breaking one of the Zr-O bonds of the cubic or tetragonal structure. The formation of cubic ZrO<sub>2</sub> at room temperature from monoclinic phase has been reported by Bid et al [9]. The three phases of ZrO<sub>2</sub> (c, t and m) occur at atmospheric pressure, but at very high pressure ZrO<sub>2</sub>

goes to orthorhombic phase [10]. Pressure-temperature phase diagram of  $ZrO_2$  at 3.8 GPa pressure and 700°C has been studied by Block et al [11]. Transformation from cubic/tetragonal to monoclinic is rapid and is accompanied by increase in volume by 3-5% that causes extensive cracking in the material. Cubic zirconia is a useful refractory and good ceramic material because it does not go through destructive phase transitions during heating and cooling. The controlled stress induced volume expansion of the cubic/tetragonal to monoclinic inversion is used to produce very high strength, hardness, tough varieties of zirconia for mechanical and structural applications [12, 13]. Double ceramic layer based zirconia was synthesized with lowest thermal diffusivity to withstand thermal cycling process [14]. Synthesis of zirconia micro needles by direct nucleation of particles inside hexagonal swollen liquid crystals was reported by Santos et al [15]. Monoclinic  $ZrO_2$  was synthesized using chemical precipitation and hydrothermal methods and its electronic structure, optical and dielectric properties were studied [16, 17]. Synthesis of nanofiber zirconia by ultrasonic spray pyrolysis was done and characterized using different techniques to use in various applications like fuel cells and oxygen sensors [18].

In our laboratory, free piston driven shock tube (FPST) is employed to perform shock tube experiments to study the interaction of shock heated gases with different materials like  $CeCrO_2$  [19],  $CeO_2$  [20],  $MoS_2$  [21, 22], graphitic carbon nanoparticles [23], etc. Material synthesis, phase transformation, surface modification, surface catalytic and aerothermodynamics reactions were also performed using shock tubes at different ambient conditions. Design, development and working principle of FPST were reported in the literature [24].

The objective of the present paper is to study the interaction of high-temperature ceramics with shock heated test gases using FPST. The advantage of this experimental method is that the test gases can be heated to extremely high temperatures at moderate pressures for few milliseconds using FPST. In this paper, we present the interaction of strong shock heated  $O_2$  and  $N_2$  test gases with cubic zirconia and the effect of shock on the samples were studied to understand its electronic structure, surface chemical reactions, crystalline properties and phase transformation.

## Experimental

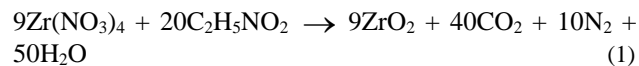
### *Materials/ chemicals details*

Zirconium nitrate ( $Zr(NO_3)_4$ ) and glycine ( $C_2H_5NO_2$ ) of analytical grade were procured commercially and used without further purification to synthesize zirconia powders by solution combustion method. Ultra-high pure (UHP) gases like  $O_2$ ,  $N_2$ , Ar, He of 99.999% purity were procured from Aditya Gas Industries, Bangalore to carry out shock tube experiments.

### *Synthesis of $ZrO_2$ by solution combustion method*

Zirconia has attracted much attention due to its scientific and technological importance and it is synthesized by various wet-chemical processes. The combustion

synthesis is attractive due to its simplicity and good laboratory technique to produce nano-crystalline powder. The process basically involves the preparation of homogeneous fuel-oxidant precursor and its exothermic decomposition [25]. The resulting  $ZrO_2$  compound is usually in the form of nanopowder. The combustion chemical reaction involves mixing of 23.3 mmoles of  $Zr(NO_3)_4$  and 56.8 mmoles of glycine dissolved in 35 ml of water to get a clear solid solution. It was kept in the furnace at 450°C in a 300 ml crystallizing dish. After dehydration, the solution is ignited into a flame, rising the temperature to about 1000°C dwelling for about 40 s. Following chemical reaction is used to synthesis  $ZrO_2$ .



The product was left for 1 hour at 500°C to remove carbonaceous impurities if any and  $ZrO_2$  was obtained as white powder. The  $ZrO_2$  powder of 0.2 g was used to prepare pellets of 10mm diameter using hydraulic press unit by applying 50 kN load for 20 minutes. These pellets were mounted at the end flange of the shock tube and experiments were performed by exposing them to strong shock in presence of  $O_2$  or  $N_2$  gas.

### *Characterization*

Characterization of  $ZrO_2$  was performed before and after exposure to shock waves. The crystalline properties of zirconia were analyzed by powder X-ray diffractometer (X-pert Philips), using  $CuK\alpha$  radiation ( $\lambda = 1.54056\text{\AA}$ ), operated at an accelerating voltage of 40 kV and an emission current of 30 mA. The XRD data were acquired over the range of  $2\theta$  from 20° and 80° with 0.01° step size. The surface morphologies and chemical compositions of the  $ZrO_2$  pellets were examined by scanning electron microscope (SEM, Philips SIRION with EDS) operating at an accelerating voltage of 20 kV. Energy dispersive spectroscopy (EDS) available in the SEM was used for elemental analysis before and after exposure to shock wave. Electronic structure of  $ZrO_2$  was characterized by X-ray photoelectron spectroscopy (XPS) using  $AlK\alpha$  radiation (1486.6 eV) where C1s peak at 284.6 eV was taken as reference (ESCA-3 Mark II spectrometer, VG Scientific) and the accuracy of the binding energy (BE) reported here was  $\pm 0.1$  eV. The samples were made into pellets by adding KBr to record IR spectra from 300 to 1400  $cm^{-1}$  using Fourier transform infrared (FTIR) spectrometer (Perkin Elmer, SPECTRUM-1000).

### *Shock tube experiments*

Free piston driven shock tube (FPST), named HST3, fabricated at Aerospace Engineering department of the Institute was used to perform shock tube experiments [26]. It consists of a high pressure gas reservoir, compression tube filled with driver gas (Helium), the shock tube filled with driven gas or test gas ( $O_2$  or  $N_2$ ). Provisions for mounting  $ZrO_2$  pellet samples were made at the end flange of the driven section of the shock tube. The schematic diagram of a FPST is shown in Fig. 1(a).

The shock tube is connected to a vacuum system and provision has been made to fill test gas at a required pressure. The piston has been placed at mounting location of the gas reservoir and the piston is held rigidly by vacuum after evacuation. Aluminum diaphragm is placed between the compression tube and the shock tube. The shock tube is initially evacuated to high vacuum and UHP test gas ( $O_2$  or  $N_2$ ) is purged for number of times and then filled with required gas pressure. Sudden supply of the high-pressure gas by opening valves behind the piston sets its motion in the compression tube and as a result, the piston travels inside the compression tube with maximum velocity.

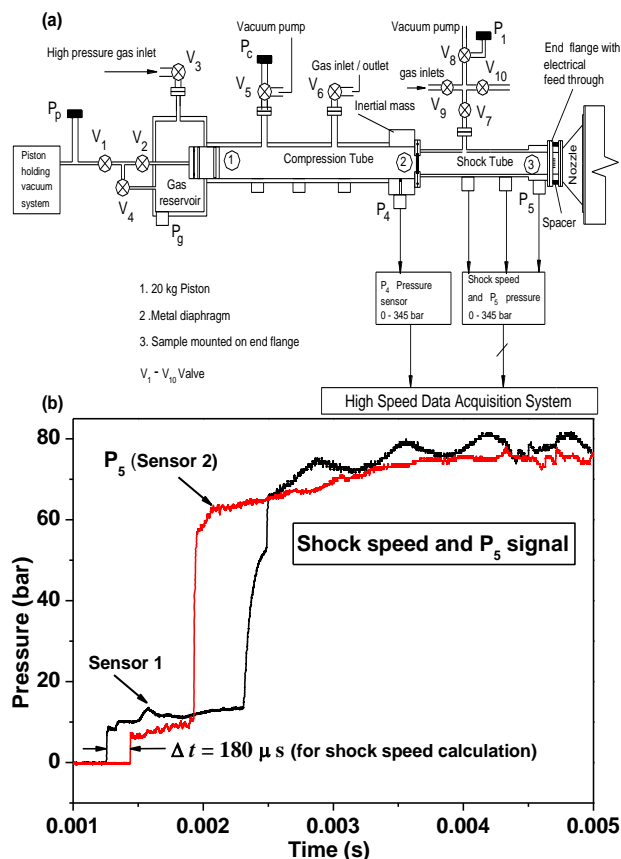


**Fig. 1.** (a) Schematic diagram of free piston driven shock tube (FPST); (b) Experimentally recorded shock time interval between sensors 1 and 2 ( $\Delta t = 180 \mu s$ ) and reflected shock pressure ( $P_5$ ) from sensor 2.

Motion of 20 kg piston inside the compression tube adiabatically compresses the helium gas and thereby increases the pressure and temperature. This high pressure and high temperature helium gas bursts the Al diaphragm at the end of the compression tube. It produces a strong shock wave, traveling into the driven section of the shock tube, which is reflected finally at the end of the shock tube to generate higher stagnation enthalpy of about 6 MJ/kg. Shock exposed test gas experiences reflected shock pressure ( $P_5$ ) and temperature ( $T_5$ ) at the end flange of the shock tube and interacts with the  $ZrO_2$  pellets.

Experimentally, the reflected shock pressure at the end of the shock tube is recorded. But reflected shock temperature ( $T_5$ ) is estimated using 1-D normal shock

relation at ambient temperature by knowing the shock Mach number ( $M_s$ ) in the driven section as follows:

$$M_s = \frac{V_s}{a_1}, \text{ where } V_s = \frac{\Delta L}{\Delta t} \quad (2)$$

where,  $\Delta L$  is the distance between the two pressure sensors,  $\Delta t$  is the time interval to travel between two sensors,  $a_1$  is the speed of sound in driven section of the shock tube and  $V_s$  is the calculated shock speed. Temperature jump across the reflected shock  $T_5$  (temperature ratio  $T_5/T_1$ , where  $T_1$  is the room temperature) is estimated using the following Rankine-Hugoniot normal shock relations [27].

$$\frac{T_5}{T_1} = \frac{\{2(\gamma-1)M_s^2 + (3-\gamma)\}\{(3\gamma-1)M_s^2 - 2(\gamma-1)\}}{(\gamma+1)^2 M_s^2} \quad (3)$$

The temperature of the test gas behind the reflected shock ( $T_5$ ) in the driven section of the shock tube is a function of shock Mach number ( $M_s$ ) of the incident shock wave and ratio of specific heat ( $\gamma$ ) of gas. The typical shock speed and reflected shock pressure ( $P_5$ ) signal are recorded using piezo electric pressure transducers for shock heated  $N_2$  experiment is shown in **Fig. 1(b)**. Experiments were carried out at 0.1 bar pressure of  $N_2$  which gives a shock Mach number of 7.4 and the corresponding reflected shock pressure and temperature are 65 bar and 7540 K (estimated) respectively. Similarly for shock heated  $O_2$  experiments, the Mach number,  $P_5$  and  $T_5$  values obtained are 8.35, 70 bar and 9530 K (estimated) respectively.

## Results and discussion

### Phase transformation from *c*- $ZrO_2$ to *m*- $ZrO_2$

XRD of zirconia pellets were recorded before and after exposure to shock waves. The characteristic diffraction line for as-prepared  $ZrO_2$  sample after assigning hkl values are shown in **Fig. 2(a)**. As-prepared sample show the diffraction line which confirms the *c*- $ZrO_2$  structure (space group  $Fm\bar{3}m$ , JCPDS no. 81-1551) with a lattice parameter ( $a$ ) of 5.152 Å. Assignment of *c*- $ZrO_2$  structure is based on XRD analysis which shows all the diffraction lines with single peak, but tetragonal structure shows all diffraction lines with double peaks. The shock treated samples in presence of oxygen gas shows *m*- $ZrO_2$  structure as shown in **Fig. 2(b)**. The cubic phase zirconia changes to *m*- $ZrO_2$  (space group  $P2_1/c$  (14), JCPDS no. 86-1451) with lattice parameters of  $a = 5.144$  Å,  $b = 5.210$  Å and  $c = 5.311$  Å and lattice angles:  $\alpha = \gamma = 90^\circ$  and  $\beta = 99.226^\circ$ . The characteristic diffraction lines are assigned with hkl values to *m*- $ZrO_2$  as shown in **Fig. 2(b)**. Surface of the pellets (about 1-2 mm thick) reacted with shock waves transforms to monoclinic phase, but diffraction lines (111) of unreacted *c*- $ZrO_2$  are indicated by (\*) as shown in **Fig. 2(b)**. XRD of as prepared  $ZrO_2$  pellet exposed to 0.1 bar  $N_2$  gas also shows

phase transformation from *c*-ZrO<sub>2</sub> to *m*-ZrO<sub>2</sub> with diffraction line (111) of unreacted *c*-ZrO<sub>2</sub> indicated by (\*) as shown in Fig. 2(c).

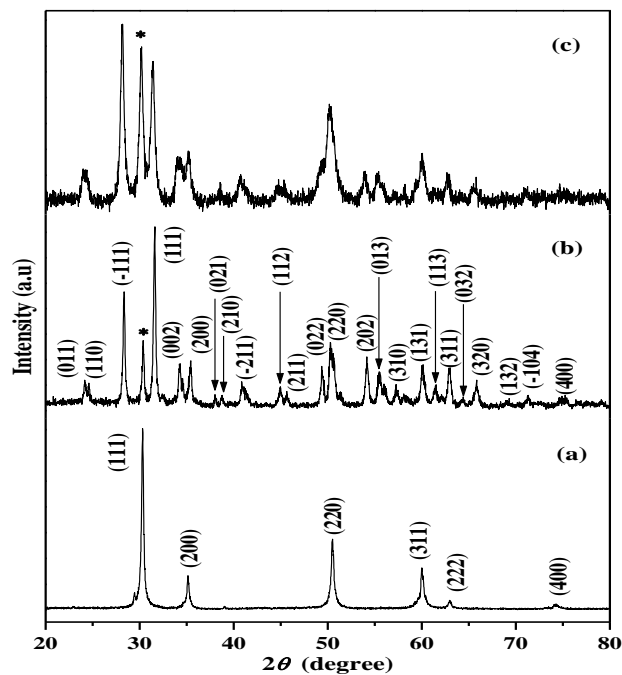


**Fig. 2.** XRD of ZrO<sub>2</sub> pellet: (a) as prepared sample showing cubic phase, (b) after subjected to shock heated 0.1 bar O<sub>2</sub> showing monoclinic phase, and (c) after subjected to shock heated 0.1 bar N<sub>2</sub> showing monoclinic phase. (\*shows presence of unreacted *c*-ZrO<sub>2</sub> sample after shock treatment).

#### Growth of nano/micro needle-like zirconia structures

SEM micrographs of as-prepared sample are shown in Fig. 3(a). For the first time using shock tube experiments, SEM micrographs show growth and formation of needle like monoclinic ZrO<sub>2</sub> structures in millisecond time scale. Needle type growth of *m*-ZrO<sub>2</sub> crystal on exposure to shock heated O<sub>2</sub> gas can be clearly seen as shown in Fig. 3(b). The growth of *m*-ZrO<sub>2</sub> needles are also observed in nitrogen shock experiment as shown in Fig. 3(c). Length of the needles varies from 2 to 10 μm with different thicknesses. Aspect ratio (length/diameter) calculated from SEM micrographs is about 15 to 20. SEM micrograph shows many needle-like crystals of small and big sizes along with the melted zirconia. Reflected shock temperature of 9530 K (estimated) interacted with *c*-ZrO<sub>2</sub> by transferring at least 2000 K within 2.0 ms test time and at about the same time it cools down and attains the room temperature. During this period *c*-ZrO<sub>2</sub> melted and recrystallized to *m*-ZrO<sub>2</sub> phase forming needle-like structure. Micrographs taken at different spots show melting of ZrO<sub>2</sub> due to super heating and the growth of needle-like structure at the tip of the melt due to super cooling in short duration at the rate of about 10<sup>6</sup> K/s. It is important to know that, in the shock tube experiment the temperature of the gas attains more than 9530 K and it remains for only 2-3 ms, after which the temperature drops down to room temperature in another 2-3 milliseconds. In all these shock tube experiments, the rise and fall in temperature is instantaneous and spontaneous.

The growth of needles from the melt occurs during the instantaneous cooling process. EDS spectra show increase in the intensity of oxygen peak due to formation of *m*-ZrO<sub>2</sub> structure and reduction of oxygen vacancy in the zirconia lattice after shock treatment with both O<sub>2</sub> and N<sub>2</sub> as shown in the insets of Fig. 3.

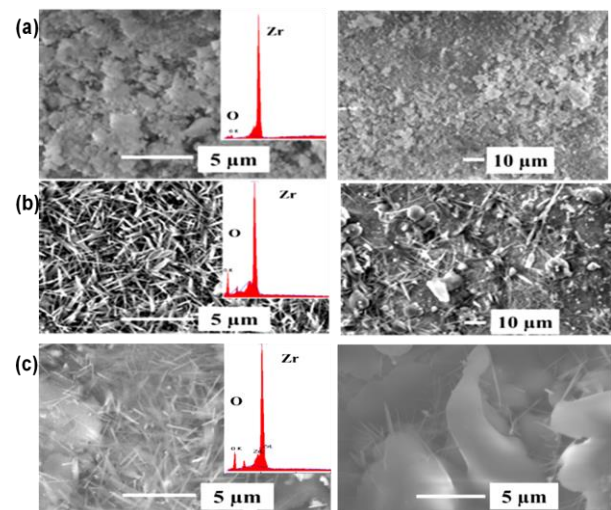


**Fig. 3.** SEM micrograph of ZrO<sub>2</sub> pellets with EDS: (a) as-prepared sample, (b) after exposed to shock at 0.1 bar O<sub>2</sub>, and (c) after exposed to shock at 0.1 bar N<sub>2</sub> (different spots shown at same magnification).

#### Electronic structure and surface chemical reactions

XPS of Zr3d core level peaks were recorded before and after exposure to shock and deconvoluted spectrum of the same are shown in Fig. 4. As-prepared *c*-ZrO<sub>2</sub> show binding energy (BE) peaks of Zr3d at 181.3 and 183.6 eV due to spin-orbit splitting of 3d<sub>5/2</sub> and 3d<sub>3/2</sub> states respectively as shown in Fig. 4(a).

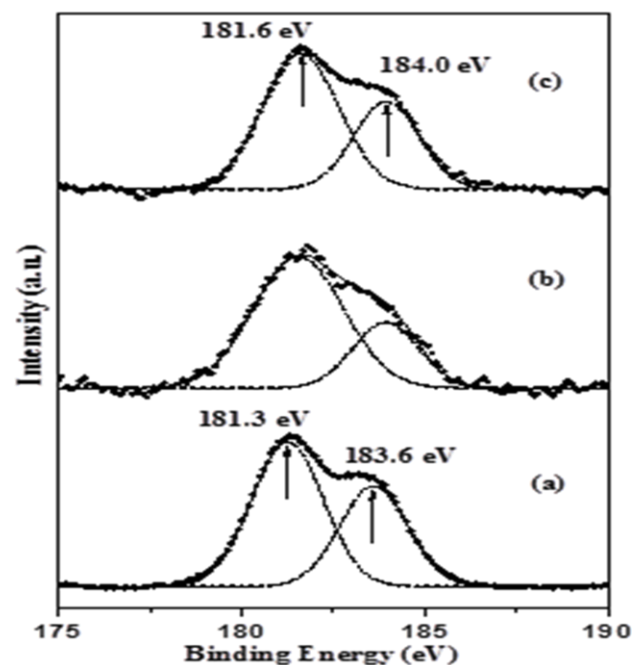


**Fig. 4.** XPS of spin-orbit splitting of Zr3d peaks: (a) as-prepared *c*-ZrO<sub>2</sub>, (b) after exposure to shock wave with 0.1 bar O<sub>2</sub> and (c) after exposure to shock wave with 0.1 bar N<sub>2</sub>.

Zr<sub>3d</sub> peaks show slight shift in BE at 181.6 and 184.0 eV due to the formation of m-ZrO<sub>2</sub> structure after exposure to shock in presence of O<sub>2</sub> and N<sub>2</sub> test gases as shown in **Fig. 4(b) and (c)** respectively. There is no change in the chemical composition of ZrO<sub>2</sub> after shock treatment which confirms the surface reaction is fully catalytic.

Surface reaction of ZrO<sub>2</sub> with shock heated oxygen gas is an endothermic process; it may be desorption of adsorbed species or due to chemical decomposition. It occurs by absorbing heat from the shockwave and by increasing the enthalpy of the system to a critical limit of its thermodynamic stability. The effect of this change can be observed with FTIR spectroscopy. FTIR spectra show the vibrational stretching frequencies of c-ZrO<sub>2</sub> and m-ZrO<sub>2</sub>, before and after shock treatment as shown in **Fig. 5**. As-prepared cubic ZrO<sub>2</sub> shows Zr-O stretching and bending vibrations between 666 and 448 cm<sup>-1</sup> as shown in **Fig. 5(a)**. Weak bands at 1192 and 1052 cm<sup>-1</sup> describe stretching vibrations of Zr=O group. After exposure to shock heated O<sub>2</sub> gas, m-ZrO<sub>2</sub> shows band between 1197 and 1063 cm<sup>-1</sup> due to Zr=O group and 735 to 375 cm<sup>-1</sup> due to Zr-O stretching and bending vibrations as shown in **Fig. 5(b)**. The relative intensity of both the phases is due to distribution of Zr<sup>4+</sup> in the crystal structure.

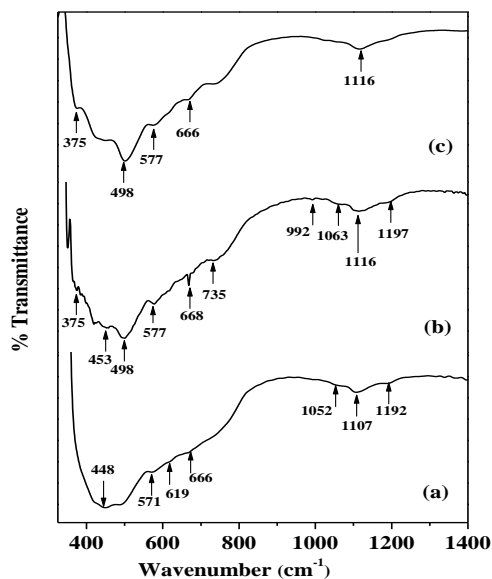


**Fig. 5.** FTIR spectra of ZrO<sub>2</sub> pellet: (a) as prepared c-ZrO<sub>2</sub>, (b) after exposure to shock wave with 0.1 bar O<sub>2</sub> and (c) after exposure to shock wave with 0.1 bar N<sub>2</sub>.

A spectrum of bands between 735 and 375 cm<sup>-1</sup> is observed in m-ZrO<sub>2</sub> in comparison with a broad unresolved band in c-ZrO<sub>2</sub> [28]. Minor variations in their band frequencies or intensities infer a small difference in the Zr<sup>4+</sup> distribution in ZrO<sub>2</sub> sites. These vibration frequencies are sensitive to oxygen vacancies, as it might have been affected due to shock in the presence of oxygen and other structural defects. Also after N<sub>2</sub> shock treatment similar bands are observed due to transformation from c-ZrO<sub>2</sub> to m-ZrO<sub>2</sub> as shown in **Fig. 5(c)**. Experimental results of both XPS and FTIR confirm that ZrO<sub>2</sub> exhibit same electronic structure and chemical composition since the surface reaction is fully catalytic.

### Fully catalytic surface recombination reaction

Experimental investigations of shock heated gas interaction on the surface of the ceramic materials are important in aerospace and other high temperature applications. Three-body catalytic surface recombination reaction occurs on the surface of c-ZrO<sub>2</sub> in presence of high temperature O<sub>2</sub> and N<sub>2</sub> gas at 9530 K and 7540 K respectively. At these temperatures, oxygen and nitrogen can go to translational, vibrational excitation and dissociation states resulting in the three-body catalytic surface recombination reaction as illustrated in **Fig. 6**.

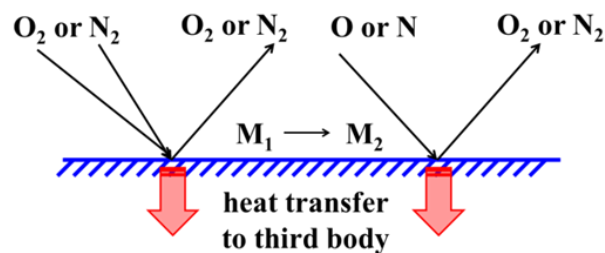


**Fig. 6.** Schematic diagram of three body catalytic surface recombination reaction.

Reactions with high temperature O<sub>2</sub>/N<sub>2</sub> (not dissociated) molecule are shown below during which heat transfers from high temperature gas to materials (third body M<sub>1</sub>):



When a shock heated O<sub>2</sub>/N<sub>2</sub> gas dissociates, the dissociated gas atoms recombine and transfer heat to the materials (third body M<sub>1</sub>) as shown in the reactions below:



where, M<sub>1</sub> is c-ZrO<sub>2</sub> and M<sub>2</sub> is m-ZrO<sub>2</sub>. In all these cases heat transfers from gas molecules to third body (M<sub>1</sub>), while the electronic structure and chemical composition of the third body remains same. From XRD and other characterization techniques, it has been concluded that ZrO<sub>2</sub> compound changes its crystal structure from cubic to monoclinic phase due to heat transfer from shock heated test gases (O<sub>2</sub> or N<sub>2</sub>). Surface heating is very high in case of catalytic wall reaction when compared to non-catalytic wall reaction [29]. ZrO<sub>2</sub> undergoes fully catalytic surface reaction which reveals that it is a promising thermal protection material for aerospace and other high temperature applications. When a space vehicle enters at a speed of 2-8 km/s, gas around the shock layer undergoes translation, vibration and dissociation states. Gas species under such conditions interact with the TBC materials which can be fully catalytic or non-catalytic surface reactions. Understanding such reaction mechanisms is of seminal importance in space applications during atmosphere re-entry.

## Conclusion

The effect of strong shock wave interaction with synthesized c-ZrO<sub>2</sub> is studied using high enthalpy shock tube in presence of O<sub>2</sub> and N<sub>2</sub> test gases. Results of this study demonstrate the change in crystal structure, decrease in oxygen vacancies, chemical composition, melting and growth of needle-like monoclinic zirconia crystals. XRD studies show as-prepared c-ZrO<sub>2</sub> sample transforms to m-ZrO<sub>2</sub> due to shock treatment. For the first time, SEM micrographs show the growth of sharp micro/nano needle-like monoclinic zirconia crystals in millisecond timescale. XPS and FTIR studies definitely demonstrate that there is no change in the electronic structure and chemical composition of ZrO<sub>2</sub> sample before and after exposure to shock waves. After examining with different experimental techniques it is confirmed that the surface reaction is fully catalytic. The effects of strong shock treatment on zirconia ceramics clearly indicate the importance of this novel experimental technique to understand the chemical and physical properties of high temperature materials. TBC materials like zirconia ceramics are used in space, nuclear and other high temperature applications, study of interaction of such materials with high temperature gases reveals some vital reaction mechanisms. This experimental methodology can be adapted to study many other high temperature materials under required aero-thermodynamic conditions using shock tubes. Moreover, the phenomenon of shock treatment in millisecond timescale needs to be analyzed by theoretical simulations to get a deeper understanding of the aero-thermochemical reactions.

## Acknowledgements

Financial supports for this study from the DST, DRDO and ISRO-IISc Space Technology Cell, Government of India are gratefully acknowledged. We are thankful to the staff at AFMM, Indian Institute of Science (IISc) for obtaining good micrographs. First author thanks Professor M S Hegde, SSCU, IISc, Bangalore for fruitful discussion and constructive comments.

## References

- Schneider, H.; Schreuer, J.; Hildmann, B; *J. Eur. Ceram. Soc.*, **2008**, 28, 329.  
DOI: [10.1016/j.jeurceramsoc.2007.03.017](https://doi.org/10.1016/j.jeurceramsoc.2007.03.017)
- Cao, X. Q.; Vassen, R.; Stoever, D; *J. Eur. Ceram. Soc.*, **2004**, 24, 1.  
DOI: [10.1016/S0955-2219\(03\)00129-8](https://doi.org/10.1016/S0955-2219(03)00129-8)
- Morinaga, M.; Adachi, H.; Tsukada, M; *J. Phys. Chem. Solids*, **1983**, 44, 301.  
DOI: [10.1016/0022-3697\(83\)90098-7](https://doi.org/10.1016/0022-3697(83)90098-7)
- Suyama, R.; Ashida, T.; Kume, S; *J. Am. Ceram. Soc.*, **1985**, 68, 314.  
DOI: [10.1111/j.1151-2916.1985.tb10130.x](https://doi.org/10.1111/j.1151-2916.1985.tb10130.x)
- Lamas, D. G.; Rosso, A. M.; Anzorena, M. S.; Frenandez, A.; Bellino, M. G.; Cabezas, M. D.; Walsoe de Reza, N. E.; Craievich A. F; *Scr. Mater.*, **2006**, 55, 553.  
DOI: [10.1016/j.scriptamat.2006.05.035](https://doi.org/10.1016/j.scriptamat.2006.05.035)
- Haines, J.; Leger, J. M.; Atouf, A. J; *J. Am. Ceram. Soc.*, **1995**, 78, 445.  
DOI: [10.1111/j.1151-2916.1995.tb08822.x](https://doi.org/10.1111/j.1151-2916.1995.tb08822.x)
- Boysen, H.; Frey, F. *Acta Crystallogr., Sect. B: Struct. Crystallogr. Cryst. Chem.*, **1991**, 47, 881.  
DOI: [10.1107/S010876819100856X](https://doi.org/10.1107/S010876819100856X)
- Martin, U.; Boysen, H.; Frey, F. *Acta Crystallogr., Sect. B: Struct. Crystallogr. Cryst. Chem.*, **1993**, 49, 403.  
DOI: [10.1107/S0108768192011297](https://doi.org/10.1107/S0108768192011297)
- Bid, S.; Pradhan, S. K; *J. Appl. Crystallogr.*, **2002**, 35, 517.  
DOI: [10.1107/S0021889802008725](https://doi.org/10.1107/S0021889802008725)
- Gateshki, M.; Petkov, V.; Williams, G.; Pradhan, S. K.; Ren, Y; *Phys. Rev. B: Condens. Matter Mater. Phys.*, **2005**, 71, 224107.  
DOI: [10.1103/PhysRevB.71.224107](https://doi.org/10.1103/PhysRevB.71.224107)
- Block, S.; Da Jornada, J. A. H.; Piermarini, G. J; *J. Am. Ceram. Soc.*, **1985**, 68, 497.  
DOI: [10.1111/j.1151-2916.1985.tb15817.x](https://doi.org/10.1111/j.1151-2916.1985.tb15817.x)
- Subbarao, E. C.; Maiti, H. S.; Srivastava, K. K; *Phys. Stat. Sol. (a)*, **1974**, 21, 9.  
DOI: [10.1002/pssa.2210210102](https://doi.org/10.1002/pssa.2210210102)
- Benali, B.; Herbst Ghysel, M.; Gallet, I.; Huntz, A. M.; Andrieux, M; *Appl. Surf. Sci.*, **2006**, 253, 1222.  
DOI: [10.1016/j.apsusc.2006.01.060](https://doi.org/10.1016/j.apsusc.2006.01.060)
- Cao, X. Q.; Vassen, R.; Tietz, F.; Stoever, D; *J. Eur. Ceram. Soc.*, **2006**, 26, 247.  
DOI: [10.1016/j.jeurceramsoc.2004.11.007](https://doi.org/10.1016/j.jeurceramsoc.2004.11.007)
- Santos, E. P.; Santilli, C. V.; Pulcinelli, S. H.; Prouzet; *E. Chem. Mater.*, **2004**, 16, 4187.  
DOI: [10.1021/cm049589h](https://doi.org/10.1021/cm049589h)
- Sharma, A.; Vrashney, M.; Kang, S.; Baik, J.; Ha, T. -K.; Chae, K. -H.; Kumar, S.; Shin, H; *J. Adv. Mat. Lett.*, **2016**, 7, 17.  
DOI: [10.5185/amlett.2016.6136](https://doi.org/10.5185/amlett.2016.6136)
- Chintaparty, R.; Reddy, N. R; *Adv. Mat. Lett.*, **2016**, 7, 235.  
DOI: [10.5185/amlett.2016.6120](https://doi.org/10.5185/amlett.2016.6120)
- Zhang, J.; Li, W.; Tanji, T; *Mater. Sci. Appl.*, **2014**, 5, 193.  
DOI: [10.4236/msa.2014.54024](https://doi.org/10.4236/msa.2014.54024)
- Jayaram, V.; Singh, P.; Reddy, K. P; *J. Appl. Mech. Mater.*, **2011**, 83, 66.  
DOI: [10.4028/www.scientific.net/AMM.83.66](https://doi.org/10.4028/www.scientific.net/AMM.83.66)
- Jayaram, V.; Gupta, A.; Reddy, K. P. J; *J. Adv. Ceram.*, **2014**, 3, 297.  
DOI: [10.1007/s40145-014-0121-1](https://doi.org/10.1007/s40145-014-0121-1)
- Brontvein, O.; Jayaram, V.; Reddy, K. P. J.; Gordon, J. M.; Tenne, R. Z; *Anorg. Allg. Chem.*, **2014**, 640, 1152.  
DOI: [10.1002/zaac.201300329](https://doi.org/10.1002/zaac.201300329)
- Vasu, K.; Matte, H. S. S. R.; Shirodkar, S. N.; Jayaram, V.; Reddy, K. P. J.; Waghmare, U. V.; Rao, C. N. R; *Chem. Phys. Lett.*, **2013**, 582, 105.  
DOI: [10.1016/j.cplett.2013.07.044](https://doi.org/10.1016/j.cplett.2013.07.044)
- Reddy, N. K.; Jayaram, V.; Arunan, E.; Kwon, Y. -B.; Moon, W. J.; Reddy, K. P; *J. Diamond Relat. Mater.*, **2013**, 35, 53.  
DOI: [10.1016/j.diamond.2013.03.005](https://doi.org/10.1016/j.diamond.2013.03.005)
- Stalker, R. J; *AAA J.*, **1967**, 5, 2160.  
DOI: [10.2514/3.4402](https://doi.org/10.2514/3.4402)
- Purohit, R. D.; Saha, S.; Tyagi, A. K; *Mater. Sci. Eng., B*, **2006**, 130, 57.  
DOI: [10.1016/j.mseb.2006.02.041](https://doi.org/10.1016/j.mseb.2006.02.041)
- Jayaram, V.D. Thesis. Bangalore (India): Indian Institute of Science, **2007**.
- Gaydon, A. G.; Hurler, I. R. *The Shock Tube in High Temperature Chemical Physics*; Reinhold Publishing Corporation: New York, **1963**.
- Mirgorodsky, A. P.; Smirnov, M. B.; Quintard, P. E; *J. Phys. Chem. Solids*, **1999**, 60, 985.  
DOI: [10.1016/S0022-3697\(99\)00005-0](https://doi.org/10.1016/S0022-3697(99)00005-0)
- Suzuki, K.; Fujita, K.; Abe, T. Chemical non-equilibrium viscous shock-layer analysis over ablating surface of super orbital re-entry capsule, In *Aerodynamics, Thermophysics, Thermal Protection, Flight System Analysis and Design of Asteroid Sample Return Capsule*; Sagami-hara, Japan, **2003**.

